

A Comparison of Sigma-Point Kalman Filters on an Aerospace Actuator

Mohammad Al Shabi^a, S. Andrew Gadsden^b, Mamdouh El Haj Assad^c and Bassam Khuwaileh^d

^a Department of Mechanical and Nuclear Engineering, University of Sharjah, PO Box 27272, Sharjah, UAE, malshabi@sharjah.ac.ae

^b College of Engineering and Physical Sciences, University of Guelph, Guelph, Ontario, Canada, N1G 2W1, gadsden@uoguelph.ca

^c Department of Sustainable & Renewable Energy Engineering, University of Sharjah, PO Box 27272, Sharjah, UAE, massad@sharjah.ac.ae

^d Department of Mechanical and Nuclear Engineering, University of Sharjah, PO Box 27272, Sharjah, UAE, bkhuwaileh@sharjah.ac.ae

ABSTRACT

This paper contains a comparison of several sigma-point Kalman filters, including the unscented Kalman filter (UKF), the cubature Kalman filter (CKF), and the central difference Kalman filter (CDKF). The comparison is based on a simulated electro-hydrostatic actuator, which is commonly used for flight surface actuation in aerospace systems. This brief study compares the response, root mean square error, and the stability of these sigma-point Kalman filters.

Keywords: Sigma point, Kalman filter, unscented, cubature, central-difference, EHA.

1. BRIEF INTRODUCTION

Estimation is the process of extracting useful information from a noisy signal. One of the most well-studied categories within estimation theory is model-based filters, which use models that mimic the system and sensor. Pioneering work in this area is nearly 60 years old, and is the well-known Kalman filter (KF). The KF is a predictor-corrector model-based filter that was developed to minimize estimation error, and is applicable on linear systems and measurements. In this case, the KF yields the optimal estimation assuming the system and measurement models are known and the respective noises are white [1-6].

When the model of the system and/or sensor are/is not linear, the traditional KF cannot be implemented. Several works were developed to modify the KF and to make it applicable to nonlinear systems. These works include the extended KF (EKF), the iterated EKF (IEKF), and higher-order EKF; where these techniques use linearization approaches such as first order Taylor series expansions and Jacobian matrices [7-10]. On the other hand, other types of KFs were developed that use statistical linearization, which is accomplished by weighted linear regression methods. These include the sigma point KF (SPKF), such as the unscented KF (UKF), the cubature KF (CKF; which is a special case of the UKF) and the central difference KF (CDKF) [11-17].

The rest of this brief paper is organized as follows. Three SPKFs are introduced in Section 2. Section 3 describes the electro-hydrostatic actuator, which is the benchmark problem of this work as it is used in aerospace applications. The results are discussed in Section 4 and are concluded Section 5.

2. THE UNSCENTED, CUBATURE AND CENTER-DIFFERENCE KALMAN FILTERS

The SPKFs linearize the models statistically using sigma points that are drawn from known distributions, and are fused together using certain weights. The UKF, CKF and CDKF are illustrated in Tables 1, 2 and 3, respectively.

Table 1. The pseudocode for the UKF code, as per [7].

$k = 0 \rightarrow \text{Initialize } \hat{\mathbf{x}}_{0 0} \text{ and } \mathbf{P}_{0 0}$ Start $k = k + 1$ for $i = 0, 1, \dots, 2n$
$\hat{\mathbf{x}}_{i_{k-1} k-1} = \hat{\mathbf{x}}_{k-1 k-1} + \begin{cases} 0 & i = 0 \\ (\sqrt{n\mathbf{P}_{k-1 k-1}})_i^T & 1 \leq i \leq n \\ -(\sqrt{n\mathbf{P}_{k-1 k-1}})_i^T & n + 1 \leq i \leq 2n \end{cases}, \hat{\mathbf{x}}_{i_{k-1} k-1} = \hat{\mathbf{f}}(\hat{\mathbf{x}}_{i_{k-1} k-1}, u_{k-1})$
end $\hat{\mathbf{x}}_{k k-1} = \sum_{i=0}^{2n} \frac{1}{2n} \hat{\mathbf{x}}_{i_{k-1} k-1}, \mathbf{P}_{k k-1} = \sum_{i=0}^{2n} \frac{1}{2n} (\hat{\mathbf{x}}_{i_{k-1} k-1} - \hat{\mathbf{x}}_{k k-1}) (\hat{\mathbf{x}}_{i_{k-1} k-1} - \hat{\mathbf{x}}_{k k-1})^T + \mathbf{Q}_{k-1}$ for $i = 0, 1, \dots, 2n$
$\hat{\mathbf{x}}_{i_{k k-1}} = \hat{\mathbf{x}}_{k k-1} + \begin{cases} 0 & i = 0 \\ (\sqrt{n\mathbf{P}_{k k-1}})_i^T & 1 \leq i \leq n \\ -(\sqrt{n\mathbf{P}_{k k-1}})_i^T & n + 1 \leq i \leq 2n \end{cases}, \hat{\mathbf{z}}_{i_{k k-1}} = \hat{\mathbf{g}}(\hat{\mathbf{x}}_{i_{k k-1}})$
end $\hat{\mathbf{z}}_{k k-1} = \sum_{i=0}^{2n} \frac{1}{2n} \hat{\mathbf{z}}_{i_{k k-1}}, \mathbf{P}_{zz} = \sum_{i=0}^{2n} \frac{1}{2n} (\hat{\mathbf{z}}_{i_{k k-1}} - \hat{\mathbf{z}}_{k k-1}) (\hat{\mathbf{z}}_{i_{k k-1}} - \hat{\mathbf{z}}_{k k-1})^T + \mathbf{R}_k$ $\mathbf{P}_{xz} = \sum_{i=0}^{2n} \frac{1}{2n} (\hat{\mathbf{x}}_{i_{k k-1}} - \hat{\mathbf{x}}_{k k-1}) (\hat{\mathbf{z}}_{i_{k k-1}} - \hat{\mathbf{z}}_{k k-1})^T$ $\mathbf{K}_k = \mathbf{P}_{xz} \mathbf{P}_{zz}^{-1}, \hat{\mathbf{x}}_{k k} = \hat{\mathbf{x}}_{k k-1} + \mathbf{K}_k (\mathbf{z}_k - \hat{\mathbf{z}}_{k k-1}), \mathbf{P}_{k k} = (\mathbf{P}_{k k-1} - \mathbf{K}_k \mathbf{P}_{zz} \mathbf{K}_k^T)$ Go back to Start

Table 2. The pseudocode for the CKF code, as per [7].

$k = 0 \rightarrow \text{Initialize } \hat{\mathbf{x}}_{0 0} \text{ and } \mathbf{P}_{0 0}$ Start $k = k + 1$ for $i = 0, 1, \dots, 2n$
$\hat{\mathbf{x}}_{i_{k-1} k-1} = \hat{\mathbf{x}}_{k-1 k-1} + \begin{cases} 0 & i = 0 \\ (\sqrt{n\mathbf{P}_{k-1 k-1}})_i^T & 1 \leq i \leq n \\ -(\sqrt{n\mathbf{P}_{k-1 k-1}})_i^T & n + 1 \leq i \leq 2n \end{cases}, \hat{\mathbf{x}}_{i_{k-1} k-1} = \hat{\mathbf{f}}(\hat{\mathbf{x}}_{i_{k-1} k-1}, u_{k-1})$
end $\hat{\mathbf{x}}_{k k-1} = \sum_{i=0}^{2n} \frac{1}{2n} \hat{\mathbf{x}}_{i_{k-1} k-1}, \mathbf{P}_{k k-1} = \frac{1}{2n} \sum_{i=1}^{2n} (\hat{\mathbf{x}}_{i_{k-1} k-1} \hat{\mathbf{x}}_{i_{k-1} k-1}^T - \hat{\mathbf{x}}_{k k-1} \hat{\mathbf{x}}_{k k-1}^T) + \mathbf{Q}_{k-1}$

for $i = 0, 1, \dots, 2n$

$$\hat{\mathbf{x}}_{i_k|k-1} = \hat{\mathbf{x}}_{k|k-1} + \begin{cases} 0 & i = 0 \\ (\sqrt{n\mathbf{P}_{k|k-1}})_i^T & 1 \leq i \leq n \\ -(\sqrt{n\mathbf{P}_{k|k-1}})_i^T & n+1 \leq i \leq 2n \end{cases}, \quad \hat{\mathbf{z}}_{i_k|k-1} = \hat{\mathbf{g}}(\hat{\mathbf{x}}_{i_k|k-1})$$

end

$$\hat{\mathbf{z}}_{k|k-1} = \sum_{i=0}^{2n} \frac{1}{2n} \hat{\mathbf{z}}_{i_k|k-1}, \quad \mathbf{P}_{zz} = \frac{1}{2n} \sum_{i=0}^{2n} (\hat{\mathbf{z}}_{i_k|k-1} \hat{\mathbf{z}}_{i_k|k-1}^T - \hat{\mathbf{z}}_{k|k-1} \hat{\mathbf{z}}_{k|k-1}^T) + \mathbf{R}_k$$

$$\mathbf{P}_{xz} = \frac{1}{2n} \sum_{i=0}^{2n} (\hat{\mathbf{x}}_{i_k|k-1} \hat{\mathbf{z}}_{i_k|k-1}^T - \hat{\mathbf{x}}_{k|k-1} \hat{\mathbf{z}}_{k|k-1}^T)$$

$$\mathbf{K}_k = \mathbf{P}_{xz} \mathbf{P}_{zz}^{-1}, \quad \hat{\mathbf{x}}_{k|k} = \hat{\mathbf{x}}_{k|k-1} + \mathbf{K}_k (\mathbf{z}_k - \hat{\mathbf{z}}_{k|k-1}), \quad \mathbf{P}_{k|k} = (\mathbf{P}_{k|k-1} - \mathbf{K}_k \mathbf{P}_{zz} \mathbf{K}_k^T)$$

Go back to Start

Table 3. Pseudocode of the CDKF from [7]

$k = 0 \rightarrow$ Initialize $\hat{\mathbf{x}}_{0|0}$ and $\mathbf{P}_{0|0}$

Start $k = k + 1$

for $i = 0, 1, \dots, 2n$

$$\hat{\mathbf{x}}_{i_{k-1}|k-1} = \hat{\mathbf{x}}_{k-1|k-1} + \begin{cases} 0 & i = 0 \\ (\sqrt{3\mathbf{P}_{k-1|k-1}})_i^T & 1 \leq i \leq n \\ -(\sqrt{3\mathbf{P}_{k-1|k-1}})_i^T & n+1 \leq i \leq 2n \end{cases}, \quad \hat{\mathbf{x}}_{i_{k-1}|k-1} = \hat{\mathbf{f}}(\hat{\mathbf{x}}_{i_{k-1}|k-1}, u_{k-1})$$

end

$$\hat{\mathbf{x}}_{k|k-1} = \sum_{i=0}^{2n} \hat{\mathbf{x}}_{i_{k-1}|k-1} \times \begin{cases} \frac{3-n}{3} & i = 0 \\ \frac{1}{6} & i \neq 0 \end{cases}, \quad \mathbf{E}_i = \hat{\mathbf{x}}_{i_{k-1}|k-1} - \hat{\mathbf{x}}_{i+n_k|k-1}, \quad \mathbf{D}_i = \hat{\mathbf{x}}_{i_{k-1}|k-1} + \hat{\mathbf{x}}_{i+n_k|k-1} - 2\hat{\mathbf{x}}_{0_k|k-1}$$

$$\mathbf{P}_{k|k-1} = \sum_{i=1}^n \frac{1}{12} \mathbf{E}_i \mathbf{E}_i^T + \sum_{i=1}^n \frac{1}{18} (\mathbf{D}_i \mathbf{D}_i^T) + \mathbf{Q}_{k-1}$$

for $i = 0, 1, \dots, 2n$

$$\hat{\mathbf{x}}_{i_k|k-1} = \hat{\mathbf{x}}_{k|k-1} + \begin{cases} 0 & i = 0 \\ (\sqrt{3\mathbf{P}_{k|k-1}})_i^T & 1 \leq i \leq n \\ -(\sqrt{3\mathbf{P}_{k|k-1}})_i^T & n+1 \leq i \leq 2n \end{cases}, \quad \hat{\mathbf{z}}_{i_k|k-1} = \hat{\mathbf{g}}(\hat{\mathbf{x}}_{i_k|k-1})$$

end

$$\hat{\mathbf{z}}_{k|k-1} = \sum_{i=0}^{2n} \hat{\mathbf{z}}_{i_k|k-1} \times \begin{cases} \frac{3-n}{3} & i = 0 \\ \frac{1}{6} & i \neq 0 \end{cases}, \quad \mathbf{E}_i = \hat{\mathbf{z}}_{i_k|k-1} - \hat{\mathbf{z}}_{i+n_k|k-1}, \quad \mathbf{D}_i = \hat{\mathbf{z}}_{i_k|k-1} + \hat{\mathbf{z}}_{i+n_k|k-1} - 2\hat{\mathbf{z}}_{0_k|k-1}$$

$$\mathbf{P}_{zz} = \sum_{i=1}^n \frac{1}{12} \mathbf{E}_i \mathbf{E}_i^T + \sum_{i=1}^n \frac{1}{18} (\mathbf{D}_i \mathbf{D}_i^T) + \mathbf{R}_k, \quad \mathbf{P}_{xz} = \frac{1}{2} \sqrt{\frac{\mathbf{P}_{k|k-1}}{3}} \left(\begin{bmatrix} \hat{\mathbf{z}}_{1_k|k-1}^T \\ \vdots \\ \hat{\mathbf{z}}_{n_k|k-1}^T \end{bmatrix} - \begin{bmatrix} \hat{\mathbf{z}}_{1+n_k|k-1}^T \\ \vdots \\ \hat{\mathbf{z}}_{2n_k|k-1}^T \end{bmatrix} \right)$$

$$\mathbf{K}_k = \mathbf{P}_{xz} \mathbf{P}_{zz}^{-1}, \quad \hat{\mathbf{x}}_{k|k} = \hat{\mathbf{x}}_{k|k-1} + \mathbf{K}_k (\mathbf{z}_k - \hat{\mathbf{z}}_{k|k-1}), \quad \mathbf{P}_{k|k} = (\mathbf{P}_{k|k-1} - \mathbf{K}_k \mathbf{P}_{zz} \mathbf{K}_k^T)$$

3. MATHEMATICAL MODELS FOR THE EHA STUDY

In this section, the aforementioned algorithms are applied to the electro-hydrostatic actuator (EHA) shown in Fig. 1. This type of device is used in several applications including aerospace for flight surface actuation. It is used to control components of a wing including the spoiler, aileron, flaps, elevator, and rudder [18]. The EHA model equations are defined as follows [18][19]:

$$\mathbf{x}_{k+1} = \begin{bmatrix} x_1 + T_s x_2 \\ x_2 + T_s x_3 \\ x_3 - T_s \left[\begin{array}{l} \frac{a_2 V_0 + M \beta_e L}{M V_0} x_3 + \frac{(A_E^2 + a_2 L) \beta_e}{M V_0} x_2 \\ + \frac{2 a_1 V_0 x_2 x_3 + \beta_e L (a_1 x_2^2 + a_3)}{M V_0} \text{sgn}(x_2) \\ \frac{1}{A_E} (a_2 x_2 + (a_1 x_2^2 + a_3) \text{sgn}(x_2)) \end{array} \right] + T_s \frac{A_E \beta_e}{M V_0} u_k \end{bmatrix}_k \quad (1)$$

Where we have the following

T_s	0.001 sec	M	7.3760	a_1	83108
A_E	1.52×10^{-3}	β_e	2.07×10^8	a_2	2100
V_0	1.08×10^{-3}	L	4.8×10^{-12}	a_3	512

In this case, the first and fourth states (position and differential pressure) are measured.

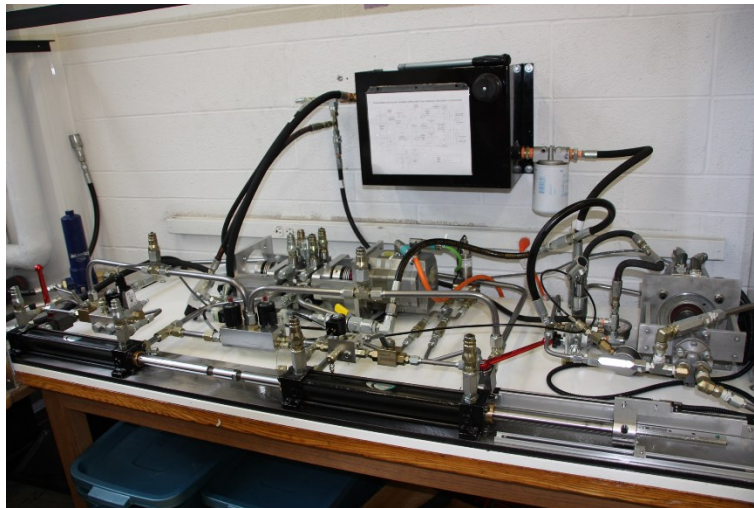


Figure 1. The EHA experimental setup at McMaster University [18][19].

4. SIMULATION RESULTS

The setup from Section 3 was used. The sampling time was 0.1 seconds. Four scenarios are considered:

1. Case 1: No modeling uncertainties and low noise level.
2. Case 2: No modeling uncertainties and high noise level.
3. Case 3: With modeling uncertainties (assuming β_e is 5000 times its value) and low noise level.
4. Case 4: With modeling uncertainties (assuming β_e is 5000 times its value) and high noise level.

The results of these cases are presented in Tables 4 to 7, and Figures 2 to 5. The results reveal that the UKF has similar results as the CKF. These two filters have superior performance compared to CDKF and EKF. Moreover, CDKF has better performance than the EKF which reinforces the fact that sigma point approximations are more accurate than linearization. Increasing the noise level makes the performance worse, particularly for the non-measured states (2 and 3). In this case, the root mean square error (RMSE) increased between 10 to 100 times. When modelling uncertainties are injected, the RMSE increased from 10 to 10^7 times which could be catastrophic for aerospace systems. This is further magnified when the noise level is increased.

Table 3. RMSE results for Case 1.

Filter	RMSE			
	Position $\times 10^{11}$	Velocity $\times 10^9$	Acceleration $\times 10^4$	Pressure $\times 10^4$
EKF	2.63	67.2	56.9	1.92
UKF	2.47	1.63	1.46	1.92
CKF	2.47	1.63	1.46	1.92
CDKF	2.48	1.50	1.58	1.92

Table 4. RMSE results for Case 2.

Filter	RMSE			
	Position $\times 10^9$	Velocity $\times 10^7$	Acceleration $\times 10^3$	Pressure $\times 10^2$
EKF	7.23	12.0	4.73	1.92
UKF	7.23	3.48	1.31	1.92
CKF	7.23	3.48	1.31	1.92
CDKF	7.22	3.48	1.32	1.92

Table 3. RMSE results for Case 3.

Filter	RMSE			
	Position $\times 10^{10}$	Velocity $\times 10^5$	Acceleration $\times 10^{-3}$	Pressure $\times 10^4$
EKF	4.32	8.22	3.84	1.92
UKF	4.34	8.47	3.07	1.92
CKF	4.34	8.47	3.07	1.92
CDKF	4.34	8.47	3.07	1.92

Table 4. RMSE results for Case 4.

Filter	RMSE			
	Position $\times 10^9$	Velocity $\times 10^4$	Acceleration $\times 10^{-3}$	Pressure $\times 10^2$
EKF	2.27	1.30	3.88	1.92
UKF	2.27	1.35	3.09	1.92
CKF	2.27	1.35	3.09	1.92
CDKF	2.27	1.35	3.09	1.92

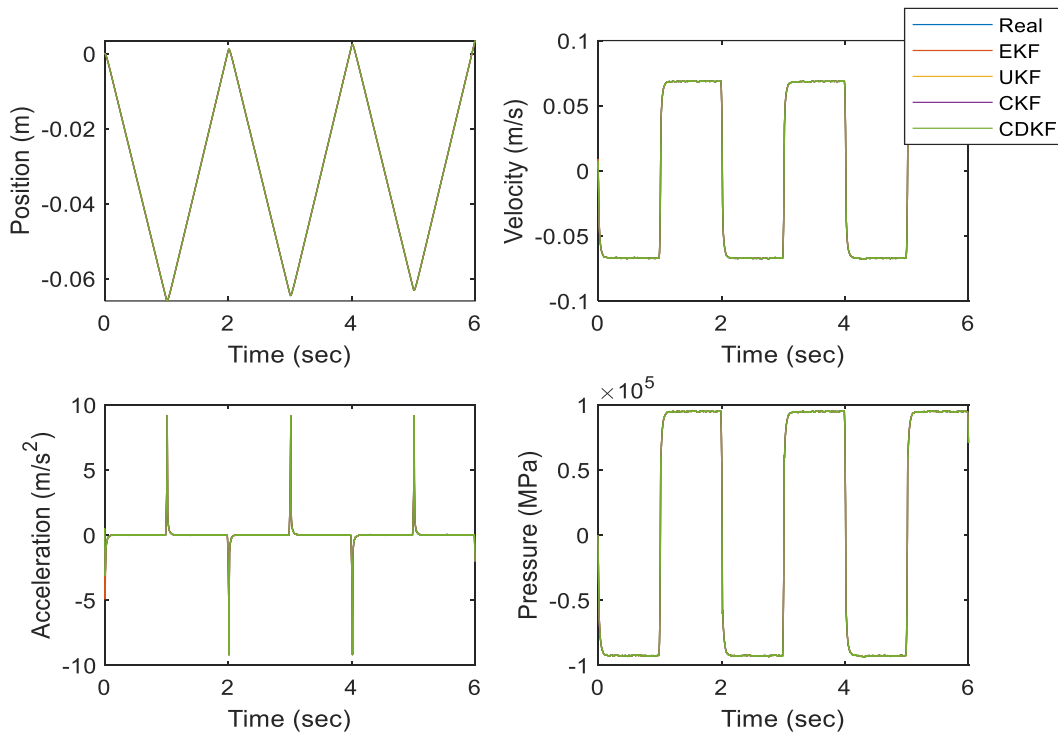


Figure 2. State estimation for Case 1.

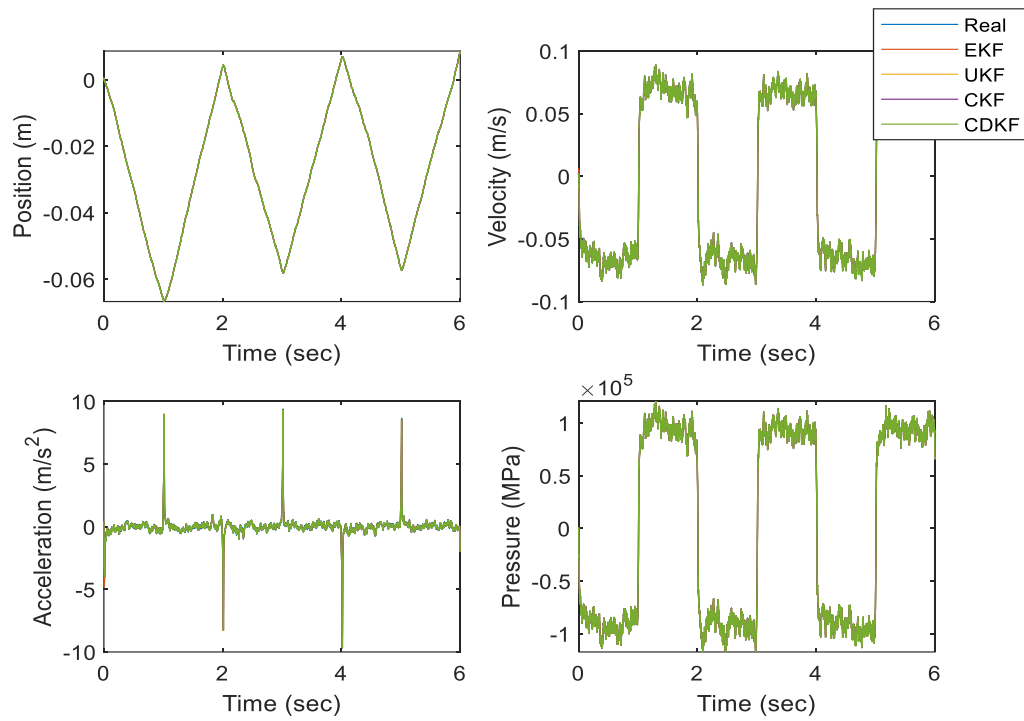


Figure 3. State estimation for Case 2.

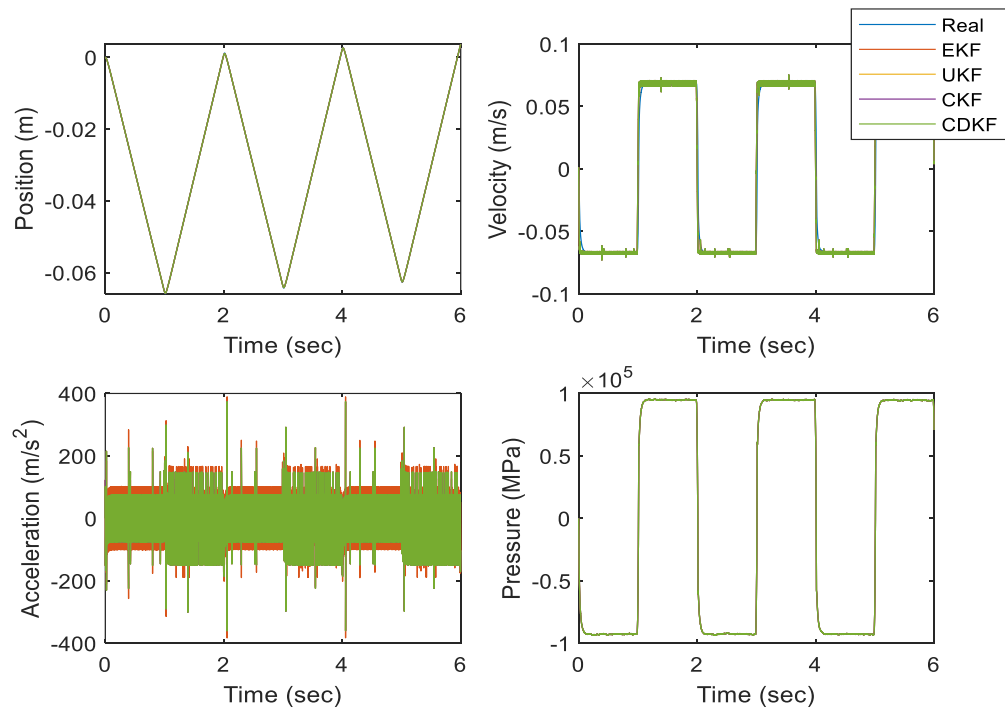


Figure 4. State estimation for Case 3.

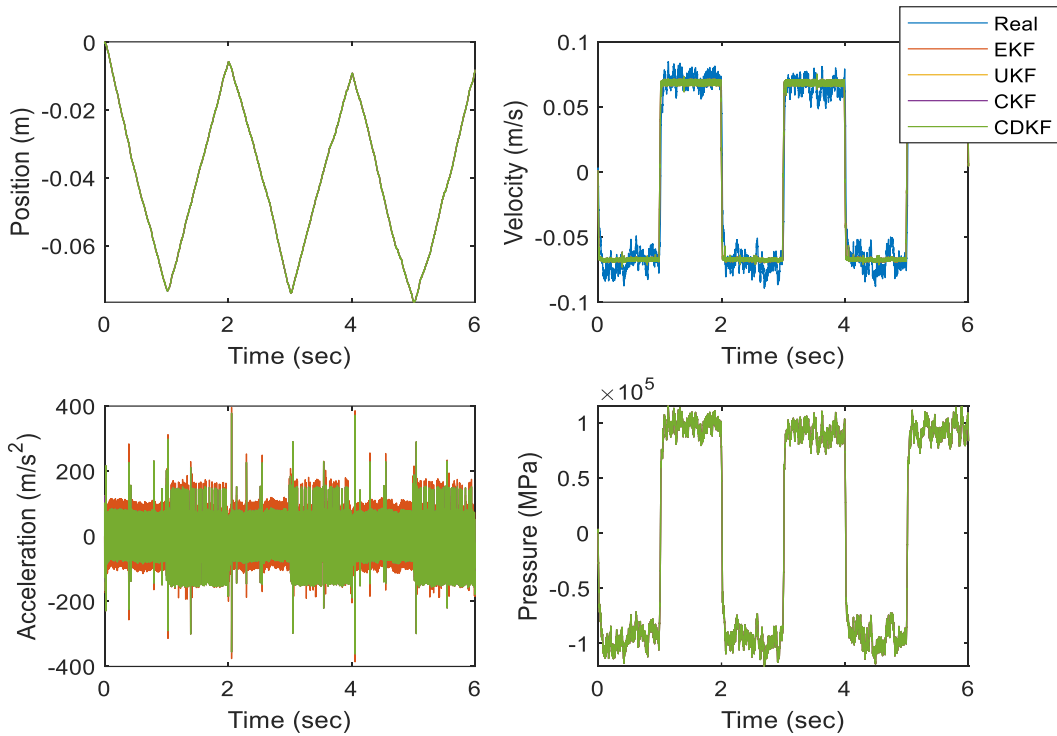


Figure 5. State estimation for Case 4.

5. CONCLUSIONS

In this work, a comparison between UKF, CKF, CDKF and EKF estimation strategies was conducted. A simulation based on a real experiment setup of the EHA was used as a benchmark problem. The results of the simulation demonstrate that all four filters were able to successfully estimate the states given a known input. The UKF and CKF yielded similar performances and they provided the best estimates among the other filters. This was followed by CDKF and then finally EKF. When modeling uncertainties were injected, the error significantly increased. Future work will look at studying these filters as applied on an experimental setup.

6. APPENDIX

The following table summarizes the main nomenclature used in this paper.

Table 5. List of nomenclature [18][19].

$^{-1} \ T$	Inverse, and transpose, respectively.	\mathbf{P}_{zz}	The output's error covariance matrix.
$(\mathbf{a})_i$	The i row of \mathbf{a} .	\mathbf{P}	The error covariance matrix.
\mathbf{e}_m	The estimation error vectors in \mathbf{m} .	q	The number of the sigma points.
$\mathbf{f}(\cdot)$	The system's model function.	\mathbf{Q}	The process noise covariance matrix.
$\mathbf{g}(\cdot)$	The sensor's model function.	\mathbf{R}	The measurements noise covariance matrix.

i, j	Subscripts used to identify elements.	Σ	The summation operator.
$\mathbf{I}_{n \times n}$	The identity matrix with dimensions of $n \times n$.	T_s	Sampling time, and is equal to 0.001 sec.
k	Time step value.	\mathbf{v}, \mathbf{w}	The measurement and system noise, respectively.
$k k-1$	The a priori value at time k.	W_i	The assigned weight.
$k k$	The a posteriori value at time k.	\mathbf{x}	The state vector.
\mathbf{K}_X	The correction gain of the filter X .	\mathbf{z}	The output vector.
m, n	Number of measurements and states, respectively.	\mathbf{X}_i and \mathbf{Z}_i	The estimate and its measurement for the i^{th} sigma point, respectively.
\mathbf{P}_{xx}	The state's error covariance matrix.		

7. REFERENCES

1. Avzayesh, M., Abdel-Hafez, M.F., Al-Masri, W.M.F., Al-Shabi, M., El-Hag, A.H. A Hybrid Estimation-Based Technique for Partial Discharge Localization. (2020) IEEE Transactions on Instrumentation and Measurement, 69 (11), art. no. 9104966, pp. 8744-8753. DOI: 10.1109/TIM.2020.2999165
2. Spotts, I., Brodie, C.H., Gadsden, S.A., Al-Shabi, M., Collie, C.M. Comparison of nonlinear filtering techniques for photonic systems with blackbody radiation. (2020) Applied Optics, 59 (30), pp. 9303-9312. DOI: 10.1364/AO.403484
3. Andrew Gadsden, S., Al-Shabi, M. A study of variable structure and sliding mode filters for robust estimation of mechatronic systems. (2020) IEMTRONICS 2020 - International IOT, Electronics and Mechatronics Conference, Proceedings, art. no. 9216381. DOI: 10.1109/IEMTRONICS51293.2020.9216381
4. Lee, A.S., Andrew Gadsden, S., Al-Shabi, M. Application of nonlinear estimation strategies on a magnetorheological suspension system with skyhook control. (2020) IEMTRONICS 2020 - International IOT, Electronics and Mechatronics Conference, Proceedings, art. no. 9216390. DOI: 10.1109/IEMTRONICS51293.2020.9216390
5. Andrew Gadsden, S., Al-Shabi, M. The Sliding Innovation Filter. (2020) IEEE Access, 8, art. no. 9096294, pp. 96129-96138. DOI: 10.1109/ACCESS.2020.2995345
6. Hill, E., Lee, A.S., Gadsden, S.A., Al-Shabi, M. Intelligent estimation strategies applied to a flight surface actuator. (2018) Proceedings - 2017 IEEE 5th International Symposium on Robotics and Intelligent Sensors, IRIS 2017, 2018-January, pp. 98-103. DOI: 10.1109/IRIS.2017.8250105
7. Al-Shabi, M., Hatamleh, K., Al Shaer, S., Salameh, I., Gadsden, S.A. A comprehensive comparison of sigma-point Kalman filters applied on a complex maneuvering road. (2016) Proceedings of SPIE - The International Society for Optical Engineering, 9842, art. no. 98421I. DOI: 10.1117/12.2224233
8. Al-Shabi, M., Gadsden, S.A., Habibi, S.R. Kalman filtering strategies utilizing the chattering effects of the smooth variable structure filter. (2013) Signal Processing, 93 (2), pp. 420-431. DOI: 10.1016/j.sigpro.2012.07.036
9. Gadsden, S.A., Al-Shabi, M., Kirubarajan, T. Two-pass smoother based on the SVSF estimation strategy. (2015) Proceedings of SPIE - The International Society for Optical Engineering, 9474, art. no. 947409. DOI: 10.1117/12.2177256
10. Gadsden, S.A., Al-Shabi, M., Kirubarajan, T. Square-root formulation of the SVSF with applications to nonlinear target tracking problems. (2015) Proceedings of SPIE - The International Society for Optical Engineering, 9474, art. no. 947408. DOI: 10.1117/12.2177226
11. Al-Shabi, M., Hatamleh, K.S., Gadsden, S.A., Soudan, B., Elnady, A. Robust nonlinear control and estimation of a PRRR robot system. (2019) International Journal of Robotics and Automation, 34 (6), pp. 632-644. DOI: 10.2316/J.2019.206-0160

12. Al-Shabi, M., Cataford, A., Gadsden, S.A. Quadrature Kalman filters with applications to robotic manipulators. (2018) Proceedings - 2017 IEEE 5th International Symposium on Robotics and Intelligent Sensors, IRIS 2017, 2018-January, pp. 117-124. DOI: 10.1109/IRIS.2017.8250108
13. Al-Shabi, M. Sigma-point Smooth Variable Structure Filters applications into robotic arm. (2017) 2017 7th International Conference on Modeling, Simulation, and Applied Optimization, ICMSAO 2017, art. no. 7934865. DOI: 10.1109/ICMSAO.2017.7934865
14. Al-Shabi, M., Bani-Yonis, M., Hatamleh, K.S. The sigma-point central difference smooth variable structure filter application into a robotic arm. (2015) 12th International Multi-Conference on Systems, Signals and Devices, SSD 2015, art. no. 7348201. DOI: 10.1109/SSD.2015.7348201
15. Al-Shabi, M., Gadsden, S.A., Wilkerson, S.A. The cubature smooth variable structure filter estimation strategy applied to a quadrotor controller. (2015) Proceedings of SPIE - The International Society for Optical Engineering, 9474, art. no. 94741I. DOI: 10.1117/12.2181250
16. Al-Shabi, M., Hatamleh, K.S. The unscented smooth variable structure filter application into a robotic arm. (2014) ASME International Mechanical Engineering Congress and Exposition, Proceedings (IMECE), 4B. DOI: 10.1115/IMECE2014-40118
17. Gadsden, S.A., Al-Shabi, M., Arasaratnam, I., Habibi, S.R. Combined cubature Kalman and smooth variable structure filtering: A robust nonlinear estimation strategy. (2014) Signal Processing, 96 (PART B), pp. 290-299. DOI: 10.1016/j.sigpro.2013.08.015
18. Gadsden, S.A., Song, Y and Habibi, S. R. Novel Model-Based Estimators for the Purposes of Fault Detection and Diagnosis. (2013), IEEE/ASME Transactions on Mechatronics, 18, no. 4, pp. 1237-1249.
19. Gadsden, S.A. Smooth Variable Structure Filtering: Theory and Applications. (2011), Thesis, McMaster University, Hamilton, Ontario, 2011.